J Mol Model (2013) 19:4521–4527
DOI 10.1007/s00894-013-1958-x

ORIGINAL PAPER

The dynamic motion of a M (M = Ca, Yb) atom inside the C_{74} (D_{3h}) cage: a relativistic DFT study

Wei Zheng · Suzhen Ren · Dongxu Tian · Ce Hao

Received: 17 April 2013 / Accepted: 22 July 2013 / Published online: 14 August 2013

Abstract The interaction between M (M=Ca, Yb) atom and C_{74} (D_{3h}) has been investigated by all electron relativistic density function theory. With the aid of the representative patch of C_{74} (D_{3h}), we studied the interaction between C_{74} (D_{3h}) and M (M=Ca, Yb) atom and obtained the interaction potential. Optimized structures show that there are three equivalent stable isomers and there is one transition state between every two stable isomers. According to the minimum energy pathway, the possible movement trajectory of M (M=Ca, Yb) atom in the C_{74} (D_{3h}) cage is explored. The calculated energy barrier for Yb atoms moving from the stable isomer to the transition state is 10.4 kcal mol^{-1} and the energy barrier for Ca atoms is 6.1 kcal mol^{-1}. The calculated NMR spectra of M@C_{74} (M=Ca, Yb) are in good agreement with the experimental data. There are nine lines in the spectra: one 1/6 intensity signal, four half intensity signals and four full intensity signals.

Keywords Dynamic NMR · Energy potential surface · M@C74 · Raman · Relativistic DFT

Introduction

Up to now, there are lots of endohedral metallofullerenes (EMFs) to be isolated. Among them, quite a few EMFs structures have been determined by NMR [1–3]. However, C_{74} is very unstable and is called a "missing fullerene", the C_{74} cage is stabilized when a divalent metal (M) is inserted in the cage, with two electrons transferred from the metal to the C_{74} cage [4]. For example, some divalent $M^{2+}@C_{74}^{2-}$ EMFs (M=Ba [5–7], Eu [8], Sm [9–11], Ca [6, 12], Sr [6, 7], or Yb [13]) have been isolated. The atom within the C_{74} (D_{3h}) cage has been assigned to $M^{2+}@C_{74}^{2-}$ by UV–VIS, Raman and EPR spectroscopy [5–14].

The position and motion of the encapsulated metal atoms are important determinants of the chemical and physical properties of EMFs. Both experimental and theoretical studies have revealed the dynamic behavior of metal atoms encapsulated in pristine and functionalized fullerene cages. Experimentally, Miyaka et al. [15] have used ^{45}Sc solution NMR spectroscopy to show the internal motion of the scandium ions in $Sc_2@C_{84}$. The two scandium ions in $Sc_2@C_{84}$ have D_{2d} symmetry and rapidly change their positions with changing temperature. Nishibori et al. [16] showed that lanthanum atoms move inside C_{82} cages and the trajectory is like a bowl or hemisphere at room temperature using the maximum entropy method (MEM). Moreover, similar dynamical motion of divalent metals in C_{74} (D_{3h}) cages has been observed. The ^{13}C NMR spectra of Ca@C74 have been measured at different temperatures and indicate that the Ca atom hops inside the D3h cage [17]. Yamada et al. [18] reported the successful synthesis of $La_2@C_{80}(CH_2)_2NTrt$, suggesting that two La atoms can rotate freely in fullerenes. Recently, ^{13}C NMR spectroscopy strongly suggests that two encapsulated Lu atoms rapidly rotate in T_d-C_{76} fullerene cage [19]. Furthermore, the motion of metal atoms inside the fullerene cages has been confirmed by theoretical studies. Andreoni et al. [20] applied ab initio molecular dynamics to La@C_{60} and obtained the dynamic trajectory of La inside C_{60}. The dynamic behavior of europium in C_{74} was investigated by semi-relativistic density-functional based tight binding calculations and molecular dynamics simulations [21] by Viezte et al. Heine et al. calculated the dynamic NMR spectra [22] of $Sc_3N@C_{80}$ using quantum Born-Oppenheimer molecular dynamics simulations, followed by DFT-NMR calculations on a large series of snapshots from the simulations. Xu et al. [4] calculated the ^{13}C NMR spectra of Yb@C_{74} and found that the motion of Yb

W. Zheng · S. Ren · D. Tian · C. Hao (✉)
State Key Laboratory of Fine Chemicals, Dalian University of Technology, Dalian 116024, People's Republic of China
e-mail: haoce@dlut.edu.cn

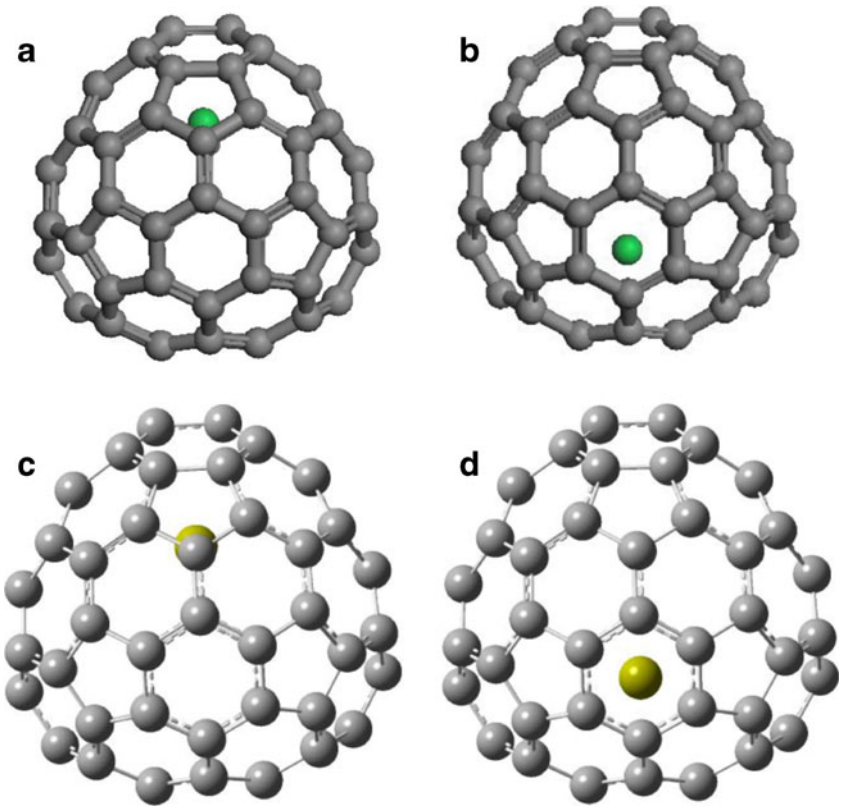

Fig. 1 All electrons relativistic DFT BLYP/DNP optimized structures of Yb@C_{74} (**a**) and transition state (**b**); Optimized structures of Ca@C_{74} (**c**) and transition state (**d**) with B3LYP/6-31G calculation

atom is similar to Ca atom in C_{74} (D_{3h}). Jin et al. showed that the La atom probably undergoes boat-shaped movement at high temperatures [23]. Zhang et al. [24] investigated La_2@C_{80} and indicated that the two La ions form a pentagonal-dodecahedral path. Recently Gan et al. performed a systematic density functional theory study on the isomers of C_{74} with 0–3 B55 bonds and 35 candidate isomers of Sc_2S@C_{74}. The results demonstrate that Sc_2S@C_{74} violates the isolated pentagon rule and its cage has two B55 bonds, the transferred electrons from Sc_2S cluster stabilize the active cage (C_{74}:13333) [25, 26].

In this study, the interaction between the M (M=Ca, Yb) atom and the C_{74} (D_{3h}) cage is analyzed considering the representative patch of C_{74} (D_{3h}). The stable point and transition state (TS) of M@C_{74} (M=Ca, Yb) are found using all electron relativistic density function theory. We analyzed the Raman spectra of M@C_{74} (M=Ca, Yb). With the aid of the potential energy surface (PES) obtained by a single point energy scan over theσ_h surface of the cage, the motion of M (M=Ca, Yb) atom in the cage is clarified. Furthermore, we obtained the trajectory of M (M=Ca, Yb) atom in the C_{74} (D_{3h}) cage respectively and forecasted the dynamic NMR spectra of M@C_{74} (M=Ca, Yb). We analyzed the dynamic motion of M (M=Ca, Yb) atom and explained the reason why M@C_{74} (M=Ca, Yb) possesses D_{3h} symmetry.

Computational details

The density functional theory (DFT) calculations of Yb@C_{74} were performed using the Dmol3 code [27, 28], firstly with the generalized gradient approximation (GGA) [29] and the Becke-Lee-Yang-Parr (BLYP) [27, 28] exchange correlation functional, which is a combination of the Becke exchange functional coupled with the Lee-Yang-Parr (LYP) correlation potential. The basis sets used in this work were double-numerical quality basis sets with polarization functions (DNP). To take into account relativistic effects [30–33], the all-electron scalar relativistic method using the Douglas-Kroll-Hess (DKH) Hamiltonian, the most accurate approach available in Dmol3, was chosen. Self-consistent field procedures

Table 1 Computed geometry parameters and energy parameters of Yb@C_{74} (C_{2v}) and Ca@C_{74} (C_{2v})

M^{2+}@C_{74}^{2-}	Structure	Relative energies[a] (kcal mol^{-1})	The distance of M-center (Å)	Number of imaginary frequencies
Yb@C_{74}	C_{2v}(a)	0	1.8	0
	C_{2v}(b)	10.4	–	1
Ca@C_{74}	C_{2v}(c)	0	1.5	0
	C_{2v}(d)	6.1	–	1

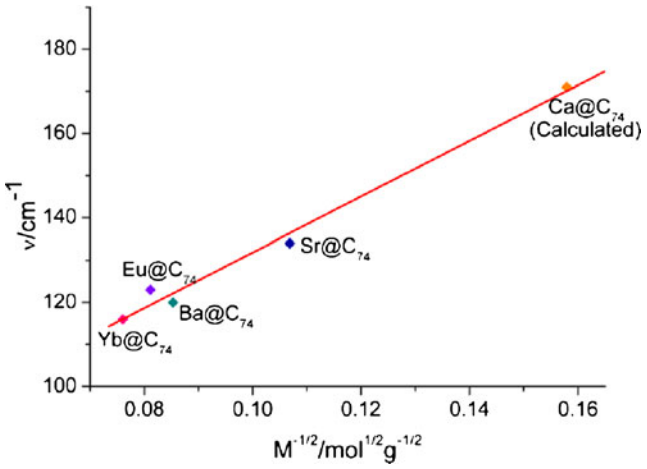

Fig. 2 Plot of the wave number of the low frequency Raman metal-cage mode vs. $M^{-1/2}$

were carried out with a convergence criterion of 10^{-6} a.u. on the energy and electron density. The full geometry optimizations were performed using the Broyden-Fletcher-Goldfarb-Shanno (BFGS) algorithm with a convergence criterion of 10^{-3} a.u. on the displacement and 10^{-5} a.u. on the energy. The transition states were searched for using the complete LST/QST [34] method with a convergence criterion of 0.002 a.u. on the RMS. The single point energy scans were carried out with the GGA functional, the BLYP correlation exchange functional, DNP basis sets, and considering relativistic effects. The ^{13}C_NMR spectrum of Yb@C74 was calculated using the ADF program [35, 36], with the generalized gradient approximation (GGA), the BLYP exchange correlation functional, and the TZP basis set.

The density functional theory (DFT) calculations of Ca@C_{74} were performed using the Gaussian 03 code [37] with the Becke-(three-parameter)-Lee-Yang-Parr (B3LYP) [30] exchange correlation functional. The full geometry optimizations were performed using the 6–31 basis sets. While the single point energy scans were carried out with the GGA functional, the BLYP correlation exchange functional, DZ basis sets. We used the same basis sets to obtain the Raman spectra and ^{13}C_NMR spectra of Ca@C_{74}.

Results and discussion

Geometry optimization and transition state of M@C_{74} (M=Ca, Yb)

Accoding to the experimental evidences [4, 17], the hollow C_{74} cage with D_{3h} symmetry was firstly optimized, and then the M (M=Ca, Yb) atom was put in the cage. To find the most stable position for the M (M=Ca, Yb) atom in C_{74}, full geometry optimizations were carried out for M@C_{74} (M=Ca, Yb), giving the most stable structure of M@C_{74} (M=Ca, Yb) shown in Fig. 1(a, c). The point group symmetry of M@C_{74} (M=Ca, Yb) reduces from D_{3h} to C_{2v} upon encapsulation of the M (M=Ca, Yb) atom. The Yb atom is located about 1.8 Å off-center and under a [6] double bond along a C_2 axis on the σ_h plane and the Ca atom is located about 1.5 Å off-center, and the global minimum was confirmed. The transition state of M@C_{74} (M=Ca, Yb) is shown in Fig. 1(b, d) and the M (M=Ca, Yb) atom is located in the opposite direction along the C_{2v} axis with the imaginary frequency of 48.9i $cm^{-1}$for Yb@C_{74} and 72i cm^{-1} for Ca@C_{74}. The optimized geometric parameters were shown in Table 1.

Raman frequency analyses

For the molecular point group C_{2v}, the 219(=3*75–6) normal modes of M@C_{74} (M=Ca, Yb) belong to the following symmetry species:

$$\Gamma = 59A_1(\text{IR},\ \text{Raman}) + 51A_2(\text{IR},\ \text{Raman}) + 55B_1(\text{IR},\ \text{Raman}) + 54B_2(\text{IR},\ \text{Raman})$$

Among all the 219 vibrational modes, 216 normal modes is the vibration of hollow C_{74} cage and three normal modes is the vibration of M-C_{74} (M=Ca, Yb).

Kuran et al. [8] studied the Raman spectra of Eu@C_{74} and point out that the observed vibrational modes can be roughly distinguished as internal cage modes between 200 cm^{-1} and

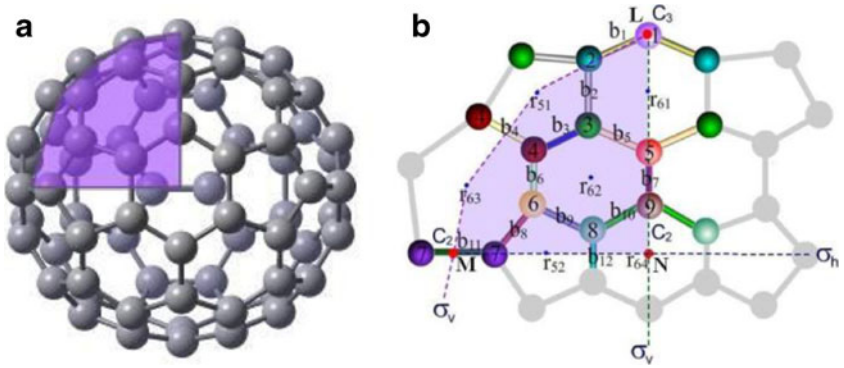

Fig. 3 Geometries of C_{74}-D_{3h} (**a**) and the representative patch of C_{74}(D_{3h}) (in the shadow) (**b**)

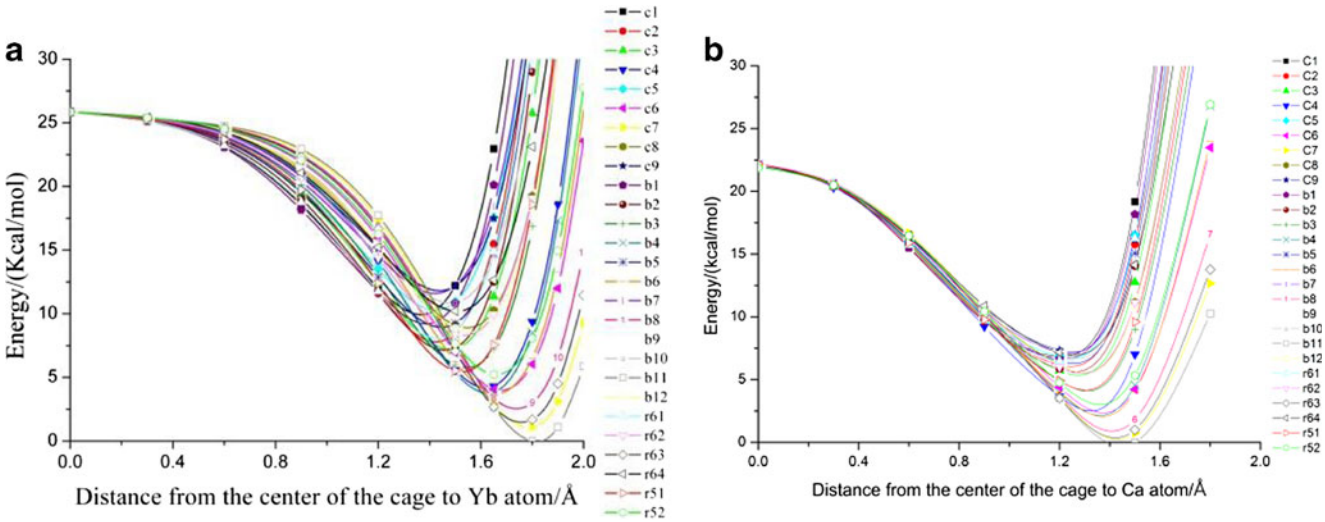

Fig. 4 Calculated potential energy curves of M atoms on the 27 key paths. (**a** Yb@C_{74}; **b** Ca@C_{74})

1600 cm^{-1} and a special (europium metal-C_{74} cage) mode at 123 cm^{-1}. In other words, only one mode in the low frequency range (<200 cm^{-1}), which may be attributed to the metal vs. cage mode. There will be no difference in the 216 normal modes of the hollow C_{74} cage. Generally speaking, there is only one peak in Raman spectra of endphedral metallofullerenes (single-metal) range from 100 cm^{-1} to 200 cm^{-1}. Since this peak is only found in endohedral metallofullerenes and relates to the motion of encapsulated metal ions in carbon cages, it has been taken as the fingerprint vibration of endohedral metallofullerenes. The experimental values are 123 cm^{-1}(Eu@C_{74}) [7, 8], 134 cm^{-1}(Sr@C_{74}) [7] and 120 cm^{-1}(Ba@C_{74}) [8] respectively. We computed the values are 171 cm^{-1}(Ca@C_{74}) and 117 cm^{-1}(Yb@C_{74}). The plot of the wave numbers of the metal vs. cage Raman mode below 200 cm^{-1} versus the square root of the reciprocal mass of the enclosed metal of the endohedral fullerenes was show in Fig. 2. A linear function representing all data points has been found and it indicates a nearly identical force constant between the metal ion and the charged cage.

The interaction between M (M=Ca, Yb) and C_{74} (D_{3h})

A representative patch for C_{74} (D_{3h})

C_{74} fullerene has only one isomer that satisfies the isolated pentagon rule with D_{3h} symmetry. To describe the symmetry of a C_{74} (D_{3h}) cage more simply, we took a right angle patch under a circum-spherical surface as being a representative patch of the C_{74} (D_{3h}) cage. The representative patch is shown in Fig. 3.

The area of the patch LMN is equal to 1/12 of the total surface area. There are 27 key points on the C_{74} (D_{3h}) representative patch. Points C1 to C9 represent nine different types of carbon atoms. Points b_1 to b_{12} represent the twelve distinct C-C bonds. While r_{61} to r_{64} represent the four types of six-member rings and r_{51} to r_{52} represent the two types of five-member rings.

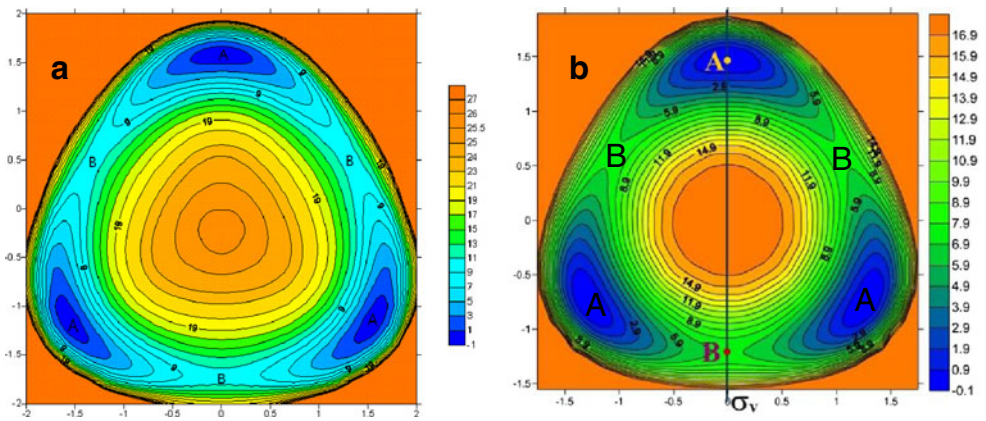

Fig. 5 The potential energy surface of Yb (**a**) and Ca (**b**) at the surface of σ_h in C_{74} (D_{3h})

The interaction between M (M= Ca, Yb) and C_{74} (D_{3h})

The interaction energy of M-C_{74} (D_{3h}) was calculated. Firstly, the C_{74} (D_{3h}) cage was fixed, and then the Yb atom and the Ca atom were allowed to approach the 27 key points along the radial directions, which pass through the center of cage and the key points. The calculated potential energy curves as a function of the distance between the M (M=Ca, Yb) atom and the key points are shown in Fig. 4.

From the graph we can see that there is a minimum energy point in each potential energy curve. These energy minima are located between 1.7 Å and 1.9 Å from the center of cage for Yb atom and 1.4 and 1.6 Å from the center of cage for Ca atom. The five minimum energy lines are C7, b_{11}, r_{52}, b_{12} and r_{64}, which are all located in the σ_h plane. To clarify the minimum energy pathway, the σ_h plane should be considered.

Using the single point energy scan, we obtained the PES of the σ_h plane. The results are shown in Fig. 5. There are three equivalent local minima on the σ_h surface of the cage along the C_2 axis, denoted by A. The transition states B are located in the opposite position with A along the C_2 axis. M (M=Ca, Yb) will need to overcome the potential barrier when it hops between the three off-center stable minima while passing through saddle point B. The relative energies between A and B are about 10 kcal mol^{-1} for Yb atom and 7 kcal mol^{-1} for Ca atom which are consistent with the value from the geometry optimization listed in Table 1. The minimum energy pathway is on the σ_h plane and it is proposed that the motion of M (M=Ca, Yb) forms a ring, which is shown in Fig. 6. Zhang et al. [23] obtained a pentagonal-dodecahedral path of La atoms in $La_2@C_{80}$ by analyzing the potential profile between different points, which is in good agreement with experiment results. That is, it is reasonable to predict the motion of the atom inside the cage by comparing the energy of different configurations.

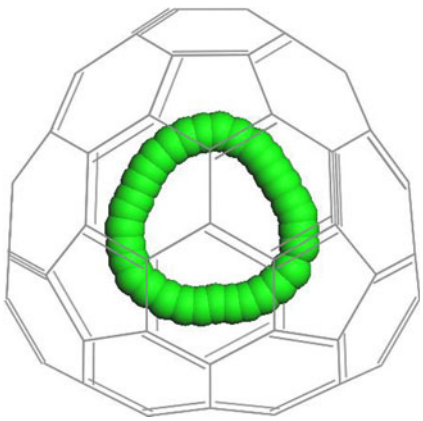

Fig. 6 The movement trajectory of M inside the C_{74} cage

Table 2 ^{13}C NMR of Yb@C_{74}

δe(ppm)[4]	δc(ppm)	Degeneracy	C
132.95	131.09	2	C1
133.41	132.89	12	C8
135.36	133.38	6	C9
137.25	134.90	12	C6
137.99	137.52	6	C5
138.45	137.55	12	C3
142.58	139.58	12	C4
145.56	141.80	6	C7
150.48	146.98	6	C2

Prediction of ^{13}C_NMR spectrum

Using the trajectory of M (M=Ca, Yb) in the C_{74} (D_{3h}) cage, the ^{13}C NMR spectrum of M@C_{74} (M=Ca, Yb) can be predicted. First, we qualitatively analyze the ^{13}C NMR of M@C_{74} (M=Ca, Yb). These should be nine lines that correspond to the nine types of atoms in the C_{74} (D_{3h}) cage. The nine carbon atoms are defined as shown in Fig. 3. We can predict the intensity of lines: C1 has C_{3v} local symmetry, so it should give 1/6 intensity signals; C2, C5, C7, C9 have C_s local symmetry, so should give half intensity signals; C3, C4, C6, C8 have C_1 local symmetry, so should give full intensity signals. In addition, we calculated the chemical shifts for all of the carbon atoms to simulate the dynamic ^{13}C_NMR spectrum of M@C_{74} (M=Ca, Yb). The 74 C atoms were divided into nine groups according to the representative path of C_{74} (D_{3h}), and their arithmetic average chemical shifts were obtained. The results are shown in Tables 2 and 3.

From Tables 2 and 3 we can see that the ^{13}C_NMR spectra are in good agreement with experimental results. For each spectrum, there are four lines with full intensity, four lines with half intensity and one line with 1/6 intensity. These NMR

Table 3 ^{13}C NMR of Ca@C_{74}

δe(ppm) [17]	δc(ppm)(this work)	I[17]	Degeneracy	C
133.6	134.35	0.4	2	C1
133.5	134.97	1.1	6	C9
135.9	136.07	1.9	12	C8
137.6	138.34	1.8	12	C6
138.3	140.02	1.0	6	C5
139.2	140.48	2.0	12	C3
143.2	142.74	1.8	12	C4
146.1	144.65	–	6	C7
150.8	151.23	1.0	6	C2

spectra indicate that M@C_{74} (M=Ca, Yb) retain the D_{3h} symmetry of the C_{74} cage.

Conclusions

Geometry optimization and vibrational frequency analysis for M@C_{74} (M=Ca, Yb) are carried out with ADF program. It is found that both configurations of the lowest energy structure and the TS of M@C_{74} (M=Ca, Yb) have C_{2v} symmetry. The energy barrier is 10.4 kcal mol^{-1} for Yb to hop from one stable site to another. While the corresponding energy barrier is 6.1 kcal mol^{-1} for Ca atom. The dynamic motion of M (M=Ca, Yb) atom in the C_{74} (D_{3h}) cage is analyzed according to the energy distribution. The lowest energy pathway is on the σ_h plane, and the trajectory is a ring with D_{3h} symmetry for M@C_{74} (M=Ca, Yb). We also calculated the Raman spectra of M@C_{74} (M=Ca, Yb) and found the values are in good agreement with the experimental results. On the basis of this, the dynamic ^{13}C NMR spectra of M@C_{74} (M=Ca, Yb) were predicted and these NMR patterns indicated that the systems have D_{3h} symmetry. This indicates that the dynamic motion of the encaged metal atom can be used to determine the dynamic motion of one or more atoms inside carbon cages.

Acknowledgments This work was supported by the National Natural Science Foundation of China (Grant Nos. 21036006 and 21137001).

References

1. Heath JR, O'Brien SC, Zhang Q, Liu Y, Curl RF (1985) Lanthanum complexes of spherical carbon shells. J Am Chem Soc 107:7779–7780
2. Chai Y, Guo T, Jin C, Haufler RE, Chibante LPF (1991) Fullerenes with metals inside. J Phys Chem 95:7564–7568
3. Nikawa H, Kikuchi T, Wakahara T, Nakahodo T, Tsuchiya T (2005) Missing metallofullerene La@C_{74}. J Am Chem Soc 127(27):9684–9685
4. Xu J, Takahiro T, Hao C, Shi Z, Wakahara T (2006) Structure determination of a missing-caged metallofullerene: Yb@C_{74} (II) and the dynamic motion of the encaged ytterbium ion. Chem Phys Lett 419:44–47
5. Haufe O, Reich A, Moschel C, Jansen M (2001) Darstellung, Isolierung und Charakterisierung von Ba@C_{74}. Z. Anorg Allg Chem 627:23–27
6. Grupp A, Haufe M, Jansen M, Mehring M, Panthofer J (2002) Synthesis, isolation and characterisation of New alkaline earth endohedral fullerenes M@C_n (M=Ca, Sr; n=74, 76). AIP Conference Proceedings 633:31–34
7. Haufe O, Hecht M, Grupp A, Mehring M, Jansen M (2005) Isolation and spectroscopic characterization of new endohedral fullerenes in the size gap of C_{74} to C_{76}. Z Anorg Allg Chem 631:126–130
8. Kuran P, Krause M, Bartl A, Dunsch L (1998) Preparation, isolation and characterisation of Eu@C_{74}:the first isolated europium endohedral fullerene. Chem Phys Lett 292:580–586
9. Okazaki T, Lian Y, Gu ZN, Suenagac K, Shinohara H (2000) Isolation and spectroscopic characterization of Sm-containing metallofullerenes. Chem Phys Lett 320:435–440
10. Okazaki T, Suenaga K, LianY GZ, Shinohara H (2001) Intrafullerene electron transfers in Sm-containing metallofullerenes:Sm@C_{2n} ($74 \leq 2n \leq 84$). J Mol Graph Model 19:244–251
11. Okazaki T, Suenaga K, Lian YF, Gu ZN, Shinohara H (2000) Direct EELS observation of the oxidation states of Sm atoms in Sm@C_{2n} metallofullerenes ($74 \leq 2n \leq 84$). J Chem Phys 113:9593–9597
12. Wan TSM, Zhang HW, Nakane T (1998) Production, isolation, and electronic properties of missing fullerenes:Ca@C72 and Ca@C74. J Am Chem Soc 120:6806–6807
13. Xu JX, Lu X, Zhou XH, He XR, Shi ZJ (2004) Synthesis, isolation, and spectroscopic characterization of ytterbium-containing metallofullerenes. Chem Mater 16:2959–2964
14. Dinadayalane TC, Leszczynski J (2010) Remarkable diversity of carbon–carbon bonds: structures and properties of fullerenes, carbon nanotubes, and grapheme. Struct Chem 21:1155–1169
15. Miyake Y, Suzuki S, Kojima Y, Kikuchi K, Kobayashi K (1996) Motion of scandium ions in Sc_2C_{84} observed by ^{45}Sc solution NMR. J Phys Chem 100:9579–9581
16. Nishibori E, Takata M, Sakata M, Tanaka H, Hasegawa M (2000) Giant motion of La atom inside C_{82} cage. Chem Phys Lett 330:497–502
17. Kodama T, Fujii R, Miyake Y, Suzuki S, Nishikawa H (2004) ^{13}C NMR study of Ca@C_{74}: the cage structure and the site-hopping motion of a Ca atom inside the cage. Chem Phys Lett 399:94–97
18. Yamada M, Wakahara T, Nakahodo T, Tsuchiya T, Maeda Y (2006) Synthesis and structural characterization of endohedral pyrrolidinodimetallofullerene: La_2@$C_{80}(CH_2)_2$NTrt. J Am Chem Soc 128:1402–1403
19. Umemoto H, Ohashi K, Inoue T, Fukui N, Sugai T (2010) Synthesis and UHV-STM observation of the T_d-symmetric Lu metallofullerene: Lu_2@$C_{76}(T_d)$. Chem Commun 46:5653–5655
20. Andreoni W, Curioni A (1996) Freedom and constraints of a metal atom encapsulated in fullerene cages. Phys Rev Lett 77:834–837
21. Vietze K, Seifert G, Fowler PW (2000) Structure and dynamics of endohedral fullerenes. AIP Conf Proc 544:131–134
22. Heine T, Vietze K, Seifert G (2004) ^{13}C NMR fingerprint characterizes long time-scale structure of Sc_3N@C_{80} endohedral fullerene. Magn Reson Chem 42:S199–S201
23. Jin P, Hao C, Li SM, Mi WH, Sun ZC (2006) Theoretical study on the motion of a La atom inside a C_{82} cage. J Phys Chem A 111:167–169
24. Zhang JF, Hao C, Li SM, Mi WH, Jin P (2007) Which configuration is more stable for La@C_{80}, D3d or D2h? recompution with ZORA methods within ADF. J Phys Chem C 111:7862–7867
25. Gan LH, Chang Q, Zhao C, Wang CR (2013) Sc2S@C74: Linear metal sulfide cluster inside an IPR-violating fullerene. Chem Phys Lett 570:121–124
26. Gan LH, An J, Pan FS, Chang Q, Liu ZH, Tao CY (2011) Geometrical and electronic rules in fullerene-based compounds. Chem Asian J 6:1304–1314
27. Delley B (1990) An all-electron numerical method for solving the local density functional for polyatomic molecules. J Chem Phys 92:508–517
28. Delley B (1990) From molecules to solids with the $DMol^3$ approach. J Chem Phys 113:7756–7764
29. Artacho E, Sànchez-Portal D, Ordejòn P, Garcla A, Soler JM (1999) Linear-scaling ab-initio calculations for large and complex systems. Phys Status Solidi (a) 215:809–817
30. Becke AD (1998) Density-functional exchange-energy approximation with correct asymptotic behavior. Phys Rev A 38:3098–3100

31. Lee C, Yang W, Parr RG (1998) Development of the Colle-Salvetti correlation-energy formula into a functional of the electron density. Phys Rev B 37:785–789
32. Powell RE (1968) Relativistic quantum chemistry. J Chem Educ 45:558–563
33. Pitzer K (1979) Relativisitic effects on chemical properties. Acc Chem Res 12:271–276
34. Pyykko P, Desclaux JP (1979) Relativity and the periodic system of elements. Acc Chem Res 12:276–281
35. Halgren TA, Lipscomb WN (1997) The synchronous-transit method for determining reaction pathways and locating molecular transition states. Chem Phys Lett 49:225–232
36. Guerra CF, Snijders JG, te Velde G, Baerends EJ (1998) Towards an order-N DFT method. Theor Chem Acc Theory Comput Model (Theoretical Chimica Acta) 99:391–403
37. te Velde G, Bickelhaupt FM, Baerends EJ, Guerra CF, van Gisbergen SJA (2001) Chemistry with ADF. J Comput Chem 22:931–967